STRUCTURAL INSTABILITY OF A BIOCHEMICAL PROCESS

V.I. GRYTSAY

Bogolyubov Institute for Theoretical Physics, Nat. Acad. of Sci. of Ukraine
(14b, Metrolohichna Str., Kyiv 03143, Ukraine)

PACS 05.45.-a, 05.45.Pq, 05.65.+b

By the example of a mathematical model of a biochemical process, the structural instability of dynamical systems is studied by calculating the full spectrum of Lyapunov indices with the use of the generalized Benettin algorithm. For the reliability of the results obtained, the higher Lyapunov index determined with the orthogonalization of perturbation vectors by the Gram–Schmidt method is compared with that determined with the overdetermination of only the norm of a perturbation vector. Specific features of these methods and the comparison of their efficiencies for a multidimensional phase space are presented. A scenario of the formation of strange attractors at a change of the dissipation parameter is studied. The main regularities and the mechanism of formation of a deterministic chaos due to the appearance of a fold or a funnel, which leads to the uncertainty of the evolution of a biosystem, are determined.

1. Introduction

One of the main physical problems is the appearance of ordered structures from the chaos in systems different by their nature due to the self-organization. The synergy was follow from theoretical physics [1]. The first model of synergy was the Turing model ("Morphogenesis model") [2]. The next was the Prigogine's "Brusselator", where self-organization regimes were considered in an abstract chemicothermal system [3]. Synergy allows one to find common physical rules for the self-organization of opened nonlinear systems [4–7].

To a significant extent, the problem concerns the question of the self-origination of life, the evolutionary development of the alive, and the basic mechanisms of structural-functional regularities of transformations in various biochemical systems. In the general case, biochemical systems are described by ordinary nonlinear differential equations of the form $\frac{d\overline{X}}{dt} = \overline{f}(\overline{X}, \overline{a})$, where $\overline{X} = (X_1, ...X_n) \in \overline{R^n}$ is a vector of variables of states (phase variables), and $\overline{a} = (a_1, ..., a_k) \in \overline{R^k})$ is the vector of parameters of the system. The results of numerical solutions of the equations can be compared with experiments and would clarify self-organization laws.

Works [8–18] considered the mathematical model of a bioreactor transforming steroids [19] under flow conditions depending on a change of the dissipation, the kinetic membrane potential of cells, and the input flows of a substrate and oxygen. Various scenarios of the transition from stationary modes to self-oscillatory modes with different multiplicities were presented, and the regions of the formation of strange attractors were determined. It is worth noting an experiment that proved the existence of self-oscillations in a population of *Arthrobacter globiformis* cells [20].

The studies were performed with the use of the method of phase portraits. The determined regions with qualitatively identical phase portraits and the points of bifurcation do not characterize the dynamics of a biosystem sufficiently completely. The most complete information about the stability of various modes is contained in the full spectrum of Lyapunov indices. But since a mathematical model of the given biochemical system contains a lot of variables and parameters, the limitations on the solution of such problems on a computer arise due to a small volume of the work memory for the processing of a matrix of small perturbations. In addition, any error made in the programming will essentially influence the overdetermination of perturbation vectors and their orthogonalization.

To attain the reliable results, we carried out the independent calculations of both the higher Lyapunov in-

dex with the same parameters, by using the Benettin algorithm with the overdetermination of only the norm of perturbation vectors, and the full spectrum of Lyapunov indices with the orthogonalization of these vectors by the Gram–Schmidt method [21–23]. The higher Lyapunov indices obtained were practically identical, which confirms the correctness of the developed computer program.

The essence of the calculation of a higher Lyapunov index with the overdetermination of only the norm of perturbation vectors consists in the determination of the evolution of an arbitrarily small deviation from a studied trajectory of the system $\lambda = \frac{1}{n\tau}\sum_{k=1}^{n} \ln \frac{\|\overline{u_k}\|}{\varepsilon}$. After each step of calculations, it is necessary to overdetermine a deviation so that its direction will remain the same, and the norm will be equal to the input value ε, namely: $\overline{u_0 k} = \frac{\varepsilon \overline{u_k}}{\|\overline{u_k}\|}$.

The algorithm of calculations of the full spectrum of Lyapunov indices consisted in the following. Taking some point on the attractor $\overline{X_0}$ as the initial one, we traced the trajectory outgoing from it and the evolution of N perturbation vectors. In our case, $N = 10$ (the number of variables of the system [18]). The initial equations of the system supplemented by 10 complexes of equations in variations were solved numerically. As the initial perturbation vectors, we set the collection of vectors $\overline{b_1^0}$, $\overline{b_2^0}$,... $\overline{b_{10}^0}$ which are mutually orthogonal and normed by one. In some time T, the trajectory arrives at a point $\overline{X}_1$, and the perturbation vectors become $\overline{b_1^1}$, $\overline{b_2^1}$,... $\overline{b_{10}^1}$, Their renormalization and orthogonalization by the Gram–Schmidt method are performed by the following scheme:

$$\overline{b_1^1} = \frac{\overline{b_1}}{\| \overline{b_1} \|},$$

$$\overline{b_2'} = \overline{b_2^0} - (\overline{b_2^0}, \overline{b_1^1})\overline{b_1^1},\ \overline{b_2^1} = \frac{\overline{b_2'}}{\| \overline{b_2'} \|},$$

$$\overline{b_3'} = \overline{b_3^0} - (\overline{b_3^0}, \overline{b_1^1})\overline{b_1^1} - (\overline{b_3^0}, \overline{b_2^1})\overline{b_2^1},\ \overline{b_3^1} = \frac{\overline{b_3'}}{\| \overline{b_3'} \|},$$

$$\overline{b_4'} = \overline{b_4^0} - (\overline{b_4^0}, \overline{b_1^1})\overline{b_1^1} - (\overline{b_4^0}, \overline{b_2^1})\overline{b_2^1} - (\overline{b_4^0}, \overline{b_3^1})\overline{b_3^1},\ \overline{b_4^1} = \frac{\overline{b_4'}}{\| \overline{b_4'} \|},$$

.....

Then the calculations are continued, by starting from the point $\overline{X}_1$ and perturbation vectors $\overline{b_1^1}$, $\overline{b_2^1}$,... $\overline{b_{10}^1}$. After the next time interval T, a new collection of perturbation vectors $\overline{b_1^2}$, $\overline{b_2^2}$,... $\overline{b_{10}^2}$ is formed and undergoes again the orthogonalization and renormalization by the above-indicated scheme. The described sequence of manipulations is repeated a sufficiently large number of times, M. In this case in the course of calculations, we evaluated the sums

$$S_1 = \sum_{i=1}^{M} \ln \| b_1'^i \|,\ S_2 = \sum_{i=1}^{M} \ln \| b_2'^i \|, ...,$$

$$S_{10} = \sum_{i=1}^{M} \ln \| b_{10}'^i \|,$$

which involve the perturbation vectors prior to the renormalization, but after the normalization. The estimation of 10 Lyapunov indices was carried out in the following way:

$$\lambda_j = \frac{S_j}{MT},\ i = 1, 2, ...10.$$

As the test calculations for the verification of a program, we reproduced the well-known results for the finite-dimensional Lorentz system.

2. Mathematical Model

A mathematical model of the process under flow conditions in a bioreactor was developed by the general scheme of metabolic processes in *Arthrobacter globiformis* cells at a transformation of steroids [8-18].

$$\frac{dG}{dt} = \frac{G_0}{N_3 + G + \gamma_2 \Psi} - l_1 V(E_1) V(G) - \alpha_3 G, \qquad (1)$$

$$\frac{dP}{dt} = l_1 V(E_1) V(G) - l_2 V(E_2) V(N) V(P) - \alpha_4 P, \qquad (2)$$

$$\frac{dB}{dt} = l_2 V(E_2) V(N) V(P) - k_1 V(\Psi) V(B) - \alpha_5 B, \qquad (3)$$

$$\frac{dN}{dt} = -l_2 V(E_2) V(P) V(N) - l_7 V(Q) V(N) +$$

$$+ k_{16} V(B) \frac{\Psi}{K_{10} + \Psi} + \frac{N_0}{N_4 + N} - \alpha_6 N, \qquad (4)$$

$$\frac{dE_1}{dt} = E_{10}\frac{G^2}{\beta_1 + G^2}\left(1 - \frac{P + mN}{N_1 + P + mN}\right) -$$

$$-l_1 V(E_1)V(G) + l_4 V(e_1)V(Q) - a_1 E_1, \quad (5)$$

$$\frac{de_1}{dt} = -l_4 V(e_1)V(Q) + l_1 V(E_1)V(G) - \alpha_1 e_1, \quad (6)$$

$$\frac{dQ}{dt} = 6lV(Q^0 + q^0 - Q)V(O_2)V^{(1)}(\Psi) -$$

$$-l_6 V(e_1)V(Q) - l_7 V(Q)V(N), \quad (7)$$

$$\frac{dO_2}{dt} = \frac{O_{20}}{N_5 + O_2} - lV(O_2)V(Q^0 + q^0 - Q)V^{(1)}(\Psi) -$$

$$-\alpha_7 O_2, \quad (8)$$

$$\frac{dE_2}{dt} = E_{20}\frac{P^2}{\beta_2 + P^2}\frac{N}{\beta + N}(1 - \frac{B}{N_2 + B} -$$

$$-l_{10}V(E_2)V(N)V(P) - \alpha_2 E_2, \quad (9)$$

$$\frac{d\Psi}{dt} = l_5 V(E_1)V(G) + l_9 V(N)V(Q) - \alpha\Psi. \quad (10)$$

where: $V(X) = X/(1+X)$; $V^{(1)}(\Psi) = 1/(1+\Psi^2)$; $V(X)$ is a function involving the adsorption of an enzyme in the region of a local bond; $V^{(1)}(\Psi)$ is a function characterizing the influence of the kinetic membrane potential on the respiratory chain. In the modeling, it is convenient to use the following dimensionless quantities [1–11] which are set as follows: $l = l_1 = k_1 = 0.2$; $l_2 = l_{10} = 0.27$; $l_5 = 0.6$; $l_4 = l_6 = 0.5$; $l_7 = 1.2$; $l_9 = 2.4$; $k_2 = 1.5$; $E_{10} = 3$; $\beta_1 = 2$; $N_1 = 0.03$; $m = 2.5$; $\alpha = 0.0033$; $a_1 = 0.007$; $\alpha_1 = 0.0068$; $E_{20} = 1.2$; $\beta = 0.01$; $\beta_2 = 1$; $N_2 = 0.03$; $\alpha_2 = 0.02$; $G_0 = 0.019$; $N_3 = 2$; $\gamma_2 = 0.2$; $\alpha_5 = 0.014$; $\alpha_3 = \alpha_4 = \alpha_6 = \alpha_7 = 0.001$; $O_{20} = 0.015$; $N_5 = 0.1$; $N_0 = 0.003$; $N_4 = 1$; $K_{10} = 0.7$.

Equations (1)–(9) describe a change in the concentrations of (1) – hydrocortisone (G); (2) – prednisolone (P); (3) – 20β-oxyderivative of prednisolone (B); (4) – reduced form of nicotinamideadeninedinucleotide (N); (5) – oxidized form of 3-ketosteroid-$\triangle$-dehydrogenase (E_1); (6) – reduced form of 3-ketosteroid-$\triangle$-dehydrogenase (e_1); (7) – oxidized form of the respiratory chain (Q); (8) – oxygen (O_2); (9) – 20β-oxysteroid-dehydrogenase (E_2). Equation (10) describes a change in the kinetic membrane potential (Ψ).

The initial parameters of the system are as follows: $G^0 = 0.17$; $P^0 = 0.844$; $B^0 = 0.439$; $N^0 = 1.789$; $E_1^0 = 0.216$; $e_1^0 = 1.835$; $Q^0 = 2.219$; $O_2^0 = 0.309$; $E_2^0 = 1.645$; $\Psi^0 = 0.300$.

The reduction of parameters of the system to dimensionless quantities is given in works [8,9]. To solve this autonomous system of nonlinear differential equations, we applied the Runge–Kutta–Merson method. The accuracy of solutions was set to be 10^{-12}. To get the reliable results, namely in order that the system, being in the initial transient state, approach the asymptotic attractor mode, we took the duration of calculations to be 100000. For this time interval, the trajectory "sticks" the corresponding attractor.

3. Results of Studies

In work [18], the diagram of states of the system in the parametric space of input flows of the substrate and oxygen was constructed. By varying the input flow, it was established that the scenario of the formation of autoperiodic and chaotic modes is regularly repeated. Numerical calculations showed that the same scenario is preserved for fixed flows, but under a change of the dissipation of a kinetic membrane potential. Such a scenario is presented in Table 1 together with the spectra of Lyapunov indices for the given modes. As the dissipation coefficient decreases from 0.84 down to 0.04131, the stationary state is destroyed, the attractor of a single-valued autoperiodic mode is formed as a result of the Andronov–Hopf bifurcation, and then the bifurcations with the doubling of the period from a single cycle to an 8-fold cycle appear. A subsequent decrease in the dissipation coefficient leads to the formation of strange attractors with the corresponding multiplicity between regular attractors. After the attainment of the 14-fold period, a single cycle is formed again, and then it passes to the stationary state. The examples of the corresponding attractors and the kinetic curves are given in Fig. 1,*a–d*. The shape of all regular attractors $n*2^0$ is analogous to those in Fig. 1,b, where $n = 1, 2, ..., 14$. Strange attractors $n * 2^\infty$, where $n = 8, 9, ..., 13$, are analogous to those in Fig. 1,*c*. It is of interest that, after the appearance of a strange attractor $13*2^\infty$ at $\alpha = 0.032160$, a regular attractor $22 * 2^\infty$ is formed (see Fig. 1,*d*), after which the attractor $14 * 2^0$ appears further. One more specific feature of the dynamics of biosystems is shown in Fig. 1,*a*. It is revealed at small input flows of the substrate and oxygen. We observe the appearance

Table 1. Full spectra of Lyapunov indices according to the scenario of the formation of attractors in the system at a change of the dissipation.

α	Attractor	λ_1	λ_2	λ_3	λ_4	λ_5	λ_6	λ_7	λ_8	λ_9	λ_{10}	Λ
0,031365	Stable	-0,000014	-0,000005	-0,003234	-0,007137	-0,025937	-0,025970	-0,081681	-0,081633	-0,171284	-0,446740	-0,843636
0,03141	$1*2^0$	0,000036	-0,000205	-0,003039	-0,007146	-0,025823	-0,025883	-0,081808	-0,081761	-0,171208	-0,448818	-0,845654
0,0321148	$1*2^\infty$	0,000138	-0,000004	-0,000052	-0,007098	-0,020347	-0,032257	-0,082552	-0,082385	-0,157747	-0,521748	-0,903948
0,03212	$14*2^0$	-0,000071	-0,000091	-0,002980	-0,007335	-0,023929	-0,028415	-0,080350	-0,081750	-0,175247	-0,498610	-0,898779
0,032161	$1*2^{22}_\infty$	0,000113	-0,000006	-0,000330	-0,007097	-0,021280	-0,031261	-0,081255	-0,082304	-0,161395	-0,521447	-0,906263
0,032165626064	$13*2^\infty$	0,000713	0,000027	-0,002070	-0,007072	-0,022286	-0,029685	-0,080862	-0,081886	-0,166210	-0,515190	-0,903522
0,03223	$13*2^1$	0,000046	0,000006	-0,003769	-0,007450	-0,023995	-0,028636	-0,079891	-0,082819	-0,176122	-0,501826	-0,904455
0,03225	$13*2^0$	0,000011	-0,000104	-0,003803	-0,007495	-0,024637	-0,028113	-0,080027	-0,083006	-0,176044	-0,502519	-0,905760
0,032276	$12*2^\infty$	0,000477	0,000071	-0,004044	-0,007566	-0,023720	-0,028704	-0,080056	-0,082627	-0,175662	-0,504774	-0,906604
0,03233	$12*2^1$	0,000071	-0,000041	-0,004121	-0,007540	-0,023572	-0,029231	-0,079729	-0,083352	-0,176959	-0,504942	-0,909416
0,032385	$12*2^0_\infty$	-0,000040	-0,000436	-0,003699	-0,007768	-0,023001	-0,029716	-0,079777	-0,084026	-0,176407	-0,506973	-0,911843
0,03239	$11*2^\infty$	0,000671	-0,000004	-0,004486	-0,007404	-0,023429	-0,029206	-0,079781	-0,082730	-0,176838	-0,510648	-0,913855
0,032516	$11*2^0_\infty$	0,000099	-0,000217	-0,004398	-0,997974	-0,023824	-0,028864	-0,079343	-0,084960	-0,176691	-0,511298	-0,917471
0,032518	$10*2^\infty$	0,000443	0,000050	-0,004732	-0,007627	-0,023636	-0,028981	-0,079623	-0,083792	-0,177700	-0,512005	-0,917602
0,032555	$10*2^0_\infty$	0,000026	-0,000016	-0,004577	-0,007610	-0,023555	-0,029628	-0,079985	-0,083775	-0,178687	-0,512677	-0,920484
0,03269	$9*2^\infty$	0,000687	-0,000065	-0,004839	-0,007895	-0,023101	-0,029568	-0,079213	-0,083703	-0,179453	-0,520902	-0,928054
0,032864	$9*2^0_\infty$	-0,000011	-0,001281	-0,003676	-0,008435	-0,023188	-0,029643	-0,080461	-0,085482	-0,178192	-0,520110	-0,930480
0,0328709	$8*2^\infty$	0,000408	-0,000084	-0,005220	-0,007637	-0,023368	-0,029846	-0,078958	-0,085451	-0,179473	-0,523591	-0,933219
0,033	$8*2^0$	0,000018	-0,000479	-0,005010	-0,008129	-0,023981	-0,029665	-0,079172	-0,086936	-0,180133	-0,524610	-0,938097
0,0331175	$7*2^0$	0,000008	-0,000054	-0,005322	-0,007784	-0,023279	-0,030628	-0,078525	-0,085849	-0,182662	-0,534263	-0,948357
0,03386	$6*2^0$	0,000009	-0,001076	-0,005427	-0,009914	-0,021305	-0,031945	-0,078692	-0,090871	-0,183080	-0,543860	-0,966161
0,03463	$5*2^0$	0,000002	-0,002315	-0,004776	-0,008582	-0,021583	-0,033047	-0,079088	-0,090756	-0,183702	-0,556392	-0,980240
0,035	$4*2^0$	0,000003	-0,001489	-0,006162	-0,008690	-0,025117	-0,031277	-0,077706	-0,093448	-0,190550	-0,579488	-1,013924
0,035632740	$3*2^0$	0,000028	-0,000847	-0,006470	-0,009006	-0,021708	-0,033915	-0,077698	-0,090781	-0,195551	-0,609383	-1,045331
0,03753	$2*2^0$	0,000005	-0,001154	-0,006768	-0,009697	-0,018585	-0,037921	-0,075991	-0,095620	-0,203197	-0,653500	-1,102427
0,04131	$1*2^0$	0,000023	-0,000910	-0,007211	-0,015665	-0,015084	-0,039323	-0,073999	-0,099042	-0,225003	-0,717604	-1,193817
0,84	Stable	-0,000061	-0,000072	-0,003564	-0,012699	-0,012727	-0,019492	-0,299446	-0,364682	-0,791531	-1,474739	-2,979013

of a strange attractor which differs from the previous ones and possesses a complicated structure. It arises regularly at various input flows on the boundary of the transition from a stationary state to $1 * 2^0$. At small input flows, in addition to oscillations due to the desynchronization of the processes of transformation and accumulation of substrates in the biosystem, there appears the desynchronization between the processes of respiration and transformation of the substrate. Two unstable points appear. The trajectories rotate chaotically around them, by passing from one center of rotation to another one. By comparing Fig. 1,*a* and Fig. 1,*c*, it is worth noting that the chaotic mode in this biosystem is formed by two means: in the first case, the attractor creates folds inside itself, whereas a funnel is formed in the second case. Due to this circumstance, the chaotic motion mixes the trajectories in the phase space.

In addition to the phase portraits, the figures show the kinetics of one of the variables of the system. It is seen that the curves differ from one another in different modes. For strange attractors, the plots represent irregular oscillations. We indicate a combination of oscillations and jumps. The figures demonstrate also the dependence of the chaotic kinetics on the initial conditions.

An important role in the analysis of the scenario of the formation of various modes is played by Lyapunov indices. For characteristic modes, Table 1 presents their full spectra λ_1, λ_2,...,λ_{10}, and the value of their sum $\Lambda = \sum_{j=1}^{10} \lambda_j$. Figure 2,a-d gives the plots of the dependence of λ_1, λ_2, λ_3, and Λ on the dissipation coefficient α in the interval from 0.0321 to 0.033.

By analyzing the results obtained, we note that all autoperiodic modes corresponding to regular attractors $n * 2^\infty$ have higher Lyapunov indices practically equal to zero. But the chaotic modes corresponding to strange attractors $n*2^\infty$ have higher Lyapunov indices which are positive and greater by one order. It is seen in Fig. 2,*a* how the "windows of periodicity" are formed at $\lambda_1 < 0$. At the given α, the regular attractors appear, whereas the strange attractors arise outside them. The most pronounced chaotic modes correspond to maximal peaks of λ_1. By the given plot, it is possible to choose beforehand the corresponding mode of functioning for a bioreactor making no calculations again.

In Fig. 2,*b*, we show the plot for the second Lyapunov index. There, λ_2 changes accordingly to λ_1. For strange attractors, $n * 2^\infty$, $\lambda_1 > 0$, whereas $\lambda_2 \approx 0$. That is, the diverging trajectories hold themselves closely to the given limiting cycle, which preserves the multiplicity of a strange attractor. The transition from the limiting cycle

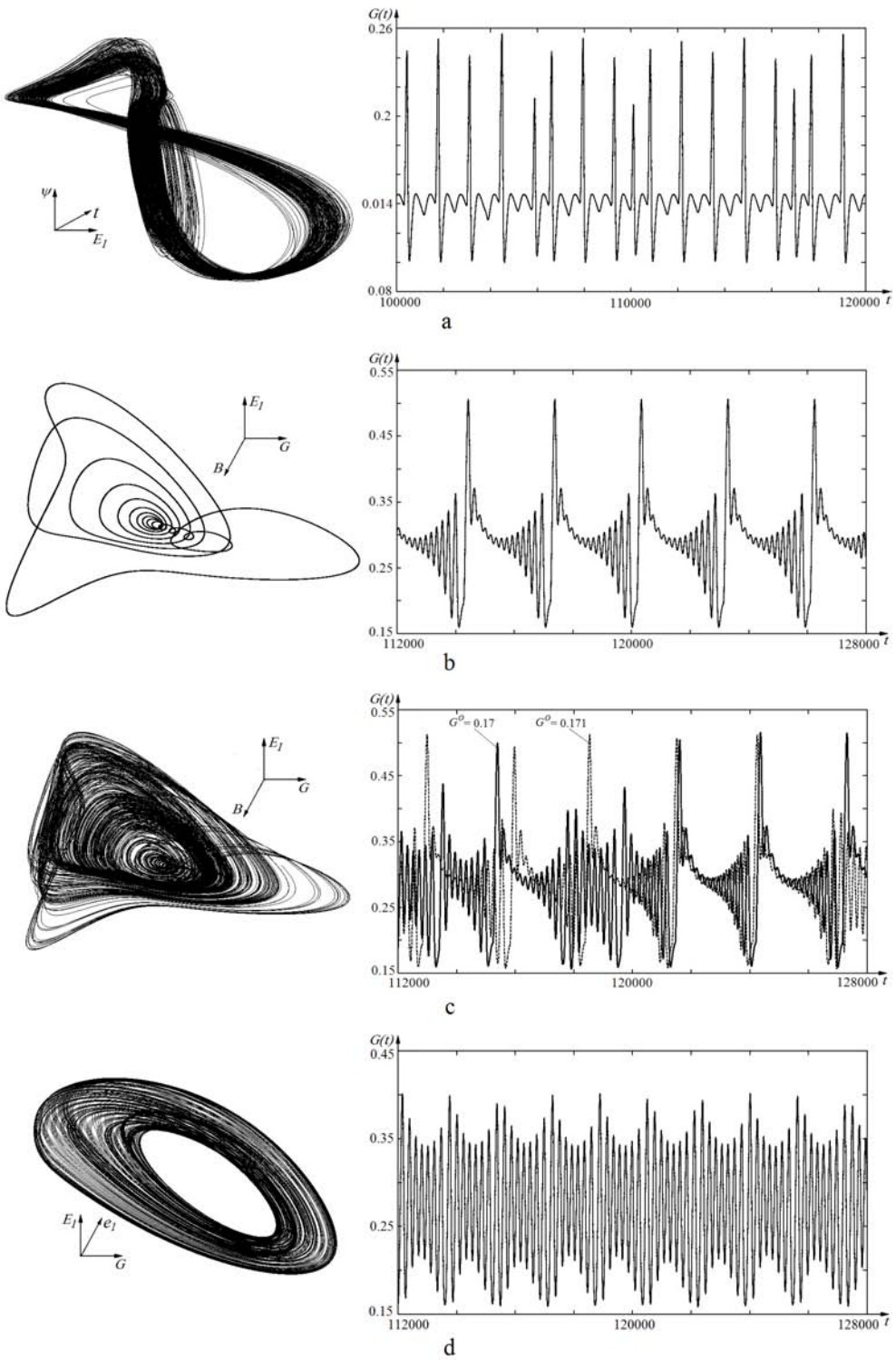

Fig. 1. Phase portraits and kinetic curves of attractors of the biosystem: *a* – strange attractor at $\alpha = 0.033$; $G_0 = 0.009$; $O_{20} = 0.00209$; *b* – regular attractor $14 * 2^0$ at $\alpha = 0.0321149$; $G_0 = 0.019$; $O_{20} = 0.015$; *c* – strange attractor $13 * 2^\infty$ at $\alpha = 0.032165626064$; $G_0 = 0.019$; $O_{20} = 0.015$; *d* – regular attractor $22 * 2^0$ at $= 0.032160$; $G_0 = 0.019$; $O_{20} = 0.015$

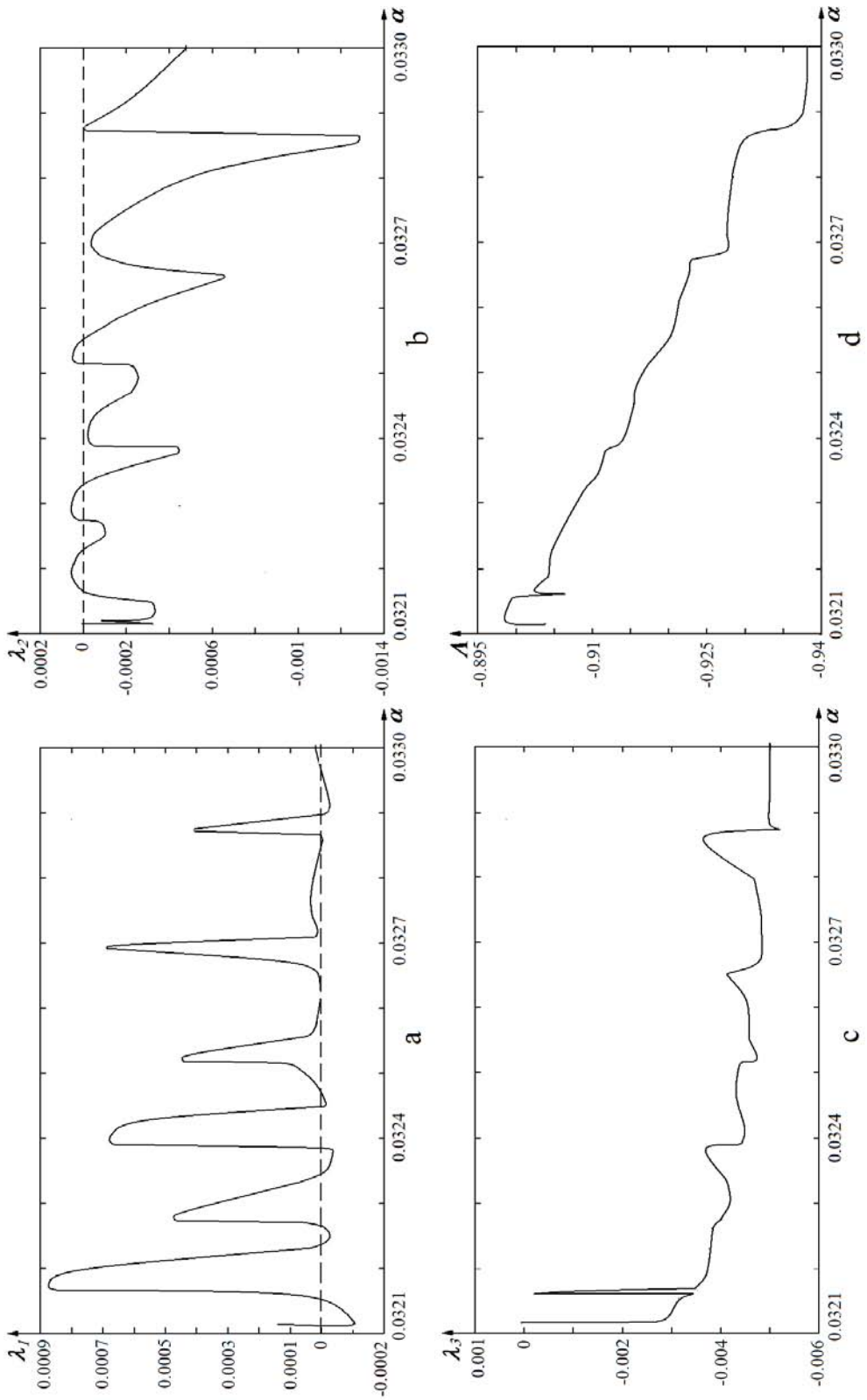

Fig. 2. Lyapunov indices versus the dissipation coefficient α: $a - \lambda_1(\alpha)$; $b - \lambda_2(\alpha)$; $c - \lambda_3(\alpha)$; $d - \Lambda(\alpha)$

to the chaotic mode occurs by means of the intermittence. The kinetics of the variable in Fig. 2,*b*, shows how the periodic limiting cycle is suddenly broken by the chaotic motion; but then the periodicity is restored again. On the phase portrait, we can separate a clearly pronounced region, whose shape is close to that of the disappeared limiting cycle, relative to which a chaotic trajectory was formed.

The variation of the third Lyapunov index is shown in Fig. 2,*c*. The behavior of λ_3 is characteristic by that this index is changed oppositely to λ_1 and λ_2. When these two indices grow, λ_3 decreases, and *vice versa*. For all α, the index λ_3 is negative.

We may imagine that a 10-dimensional parallelepiped $\overline{P}^{10}$ is constructed in the given phase space $\overline{R}^{10}$ at the beginning of a trajectory on the base of the perturbation vectors $\overline{b_1^0}$, $\overline{b_2^0}$,... $\overline{b_{10}^0}$, which are orthogonal to one another and are normed by one. The value of each index λ_j characterizes a deformation of this parallelepiped along the corresponding perturbation vector $\overline{b_1^i}$, $\overline{b_2^i}$,... $\overline{b_{10}^i}$, after i steps of the motion along the trajectory. The parallelepiped spreads along the given vector for a positive Lyapunov index and shrinks for a negative Lyapunov index.

The sum of all indices Λ as a function of α is given in Fig. 2,*d* and in Table 1. This quantity determines the flow divergence and, hence, the evolution of a phase volume along a trajectory. For the given dissipative system, the divergence is negative and increases with the growth of the dissipation α. This means that the phase volume element shrinks, on the whole, along a trajectory for all values of α. The greater the dissipation, the greater the contraction. For the regular attractors $n*2^0$, the contraction is greater than that for the corresponding strange attractor $n*2^\infty$.

Since we deal with a dissipative system, whose divergence must be negative in any modes, the phase volume must always shrink. But $\overline{b}_1^i > 0$ in the modes of a strange attractor, and there occurs the exponential spreading in this direction. Because two adjacent orbits cannot permanently exponentially diverge, the strange attractor organizes itself so that it creates a fold (Fig. 1,*a*) or a funnel (Fig. 1,*c*) in itself, where the mixing of trajectories is realized. Even a slight deviation of the initial data influences essentially the evolution of the trajectory, namely the deterministic chaos is created. Such a chaos characterizes the appearance of a random nonpredictable behavior of a system controlled by deterministic laws. We note that, in real biosystems, the fluctuations are permanently present and, in unstable modes, create chaotic states. Thus, the given mathematical model adequately describes stable autoperiodic modes, as well as unstable chaotic ones.

4. Conclusions

Due to the successful development of an algorithm of calculations of the full spectrum of Lyapunov indices on an ordinary personal computer for a multidimensional phase space not bounded by the number of variables, we manage to reliably calculate these indices. This allows one to extend the possibilities to forecast the dynamics of complicated systems. By the example of a mathematical model of biosystems, we have found two different scenarios of the formation of the modes of a strange attractor: the creation of a fold or a funnel, where the formation of a deterministic chaos is realized. The self-organization of the phase flow of a strange attractor occurs under the action of two mutually competitive processes: the exponential extension (of one of the components, in the given case) and the dissipative contraction of the whole phase space. Any fluctuation which has appeared there causes the nonpredictability of the evolution of the system on the whole.

1. L.D. Landau and E.M. Lifshitz, *Fluid Mechanics* (Pergamon Press, Oxford, 1975).
2. A.M. Turing, Phil. Trans. Roy. Soc. Lond. B **237**, 37 (1952).
3. G. Nicolis and I. Prigogine, *Self-Organization in Nonequilibrium Systems. From Dissipative Structures to Order through Fluctuations* (Wiley, New York, 1977).
4. Yu.M. Romanovskii, N.V. Stepanova, and D.S. Chernavskii, *Mathematical Biophysics* (Nauka, Moscow, 1984) (in Rissian).
5. T.S. Akhromeyeva, S.P. Kurdyumov, G.G. Malinetskii, and A.A. Samarskii, Physics Reports **176**, 189 (1989).
6. T. Reichenbach, M. Mobilia, and E. Frey, Physical Reviev E **74**, 051907 (2006).
7. J. W.Pröß, R. Schnaubelt, and R. Zacher, *Mathematische Modelle in der Biologie* (Basel, Birkhäuser, 2008).
8. V.P. Gachok, V.I. Grytsay, A.Yu. Arinbasarova, A.G. Medentsev, K.A. Koshcheyenko, and V.K. Akimenko, Biotechnology and Bioengineering **33**, 661 (1989).
9. V.P. Gachok, V.I. Grytsay, A.Yu. Arinbasarova, A.G. Medentsev, K.A. Koshcheyenko, and V.K. Akimenko, Biotechnology and Bioengineering **33**, 668 (1989).
10. V.I. Grytsay, Dopov. NAN Ukr. No 2, 175 (2000).

11. V.I. Grytsay, Dopov. NAN Ukr. No 3, 201 (2000).
12. V.I. Grytsay, Dopov. NAN Ukr. No 11, 112 (2000).
13. V.I. Grytsay, Ukr. Fiz. Zh. **46**, 124 (2001).
14. V.V. Andreev and V.I. Grytsay, Matem. Modelir. **17**, 57 (2005).
15. V.V. Andreev and V.I. Grytsay, Matem. Modelir. **17**, 3 (2005).
16. V.I. Grytsay and V.V. Andreev, Matem. Modelir. **18**, 88 (2006).
17. V.I. Grytsay, Biofiz. Visn. No 2, 25 (2008).
18. V.I. Grytsay, Biofiz. Visn. No 2, 77 (2009).
19. A.A. Akhrem and Yu.A. Titov, *Steroids and Microorganisms* (Nauka, Moscow, 1970) (in Russian).
20. A.G. Dorofeev, M.V. Glagolev, T.F. Bondarenko, and N.S. Panikov, Mikrobiol. **61**, 33 (1992).
21. I. Shimada and T. Nagashima, Progr. Theor. Phys. **61**, 1605 (1979).
22. M. Holodniok, A. Klic, M. Kubicek, M. Marek, Metody Analýzy Nelinearnich Dynamickych Modelu (Academia, Praha, 1986).
23. S.P. Kuznetsov, *Dynamical Chaos* (Nauka, Moscow, 2001) (in Russian).

Received 30.09.09

СТРУКТУРНА НЕСТІЙКІСТЬ БІОХІМІЧНОГО ПРОЦЕСУ

В.Й. Грицай

Р е з ю м е

У роботі на прикладі математичної моделі біохімічного процесу проведено дослідження структурної нестійкості динамічних систем за допомогою розрахунку повного спектра показників Ляпунова узагальненим алгоритмом Бенеттина. Для достовірності отриманих результатів проведено порівняння старших показників Ляпунова, знайдених з урахуванням ортогоналізації векторів збудження методом Грама–Шмідта, та при перевизначенні лише норми вектора збудження. Наведено особливості використання цих методів та дано їх порівняння за ефективністю для багатовимірного фазового простору. Досліджено сценарій формування дивних атракторів при зміні параметра дисипації. Знайдено основні закономірності виникнення детермінованого хаосу в системах різної фізичної природи.